TIME SERIES OBSERVATIONS OF A PHYTOPLANKTON COMMUNITY MONITORED WITH A NEW SUBMERSIBLE FLOW CYTOMETER

Heidi M. Sosik, Robert J. Olson, Michael G. Neubert,
Alexi Shalapyonok, and Andrew R. Solow
Woods Hole Oceanographic Institution, Woods Hole, MA 02543

ABSTRACT

Our understanding of the dynamics and regulation of phytoplankton communities has been limited by the space and time scales associated with traditional monitoring approaches. To overcome some of these limitations, we have developed a submersible flow cytometer (FlowCytobot) designed for extended autonomous measurements of phytoplankton abundance, cell size and pigmentation. FlowCytobot was moored on the seafloor from late July to October 2001 at the LEO-15 study site off the coast of New Jersey, and water samples from 5 m depth were pumped continuously through the instrument. The resulting measurements reveal distinct populations of *Synechococcus* and cryptophytes, as well as an assemblage of other pico- and nano-phytoplankton of mixed taxonomy. For each of these groups, dramatic variations in cell concentration were observed within the sampling period. Diel variations in cell scattering cross-section, which are indicative of changes in cell size, were consistent with patterns of cell growth during the light period and cell division late in the day. We developed a size-structured matrix population model that accommodates simultaneous growth and division, and then used the model and size distribution data from FlowCytobot to estimate daily intrinsic growth rates for *Synechococcus*; these growth rate estimates are independent of cell concentration data. The results show that a dramatic autumn decline in the concentration of *Synechococcus* was caused by a decrease in intrinsic growth rate and not by physical transport processes or trophic interactions.

INTRODUCTION

In recent decades it has become increasingly evident that marine phytoplankton are distributed in patterns that are highly variable in space and time. This evidence has come from a variety of sampling approaches ranging from shipboard- or mooring- based measurement of in vivo chlorophyll fluorescence to satellite-based assessment of ocean color (e.g., Dickey 1991; Dickey 2001). Despite these valuable measurement approaches, our knowledge of the factors that regulate phytoplankton distributions at the mesoscale and smaller continues to be limited by inadequate sampling; the outstanding problems include limited coverage and resolution in space and time as well as the need to characterize properties such as the composition, size distribution, and growth rate of the phytoplankton community.

Our recent efforts to develop an automated submersible flow cytometer ("FlowCytobot") for analysis of phytoplankton properties have been aimed at resolving some of these limitations (Olson et al. 2002). This automated sampling system, which is capable of continuously monitoring the fluorescence and light scattering of individual phytoplankton, has the potential to document changes in the taxonomic and size structure

1

of the phytoplankton community at unprecedented scales. In a moored application, such as we describe here, this kind of technology can produce time series of phytoplankton properties that reflect combined responses to biological and environmental forcing.

FLOWCYTOBOT OVERVIEW AND DEPLOYMENT

FlowCytobot is based on a 532 nm solid-state laser for excitation, combined with photomultiplier detectors for light scattering and fluorescence (Fig. 1). A sampling valve system selects from ambient seawater, and reservoirs of solutions containing detergent or standard microspheres for calibration. Sheath water is recirculated during operation. The self-contained underwater system includes signal processing electronics and a computer for sample control and data acquisition.

Figure 1. Internal view of FlowCytobot. The pressure housing endcap is on the left, fluidics and optics are in the center, and the electronics are on the right. The syringe pump and sampling valve are located over the optics and are visible near the top of the image. The optical bench rests on rubber wheels.

We deployed the FlowCytobot on the ocean bottom at the Long-term Environmental Observatory (Glenn et al. 2000) located 9 km off the coast of New Jersey (LEO-15 "Node B", 39° 27.41′ N, 74° 14.75′ W, Fig. 2) from late July to mid-October, 2001. During this deployment, power supply to the instrument, real-time data transmission to a shore-based computer, and user-initiated communication to change instrument status were accomplished via the fiber optic cable to the permanent underwater node at LEO-15. Water samples were analyzed continuously except for brief interruptions associated with data transmission problems and with scheduled communication events from the shore-based computer, which was remotely operated via the Internet.

During FlowCytobot deployment, bottom water temperature, salinity, and pressure were measured at the LEO-15 underwater nodes, surface winds and incident short wave radiation were measured at a coastal meteorological tower maintained as part of the LEO-15 observing system, and sea surface temperature data were derived from AVHRR satellite imagery. These data are available from the data management component of Rutgers University's Coastal Ocean Observation Laboratory, co-directed by S. Glenn and O. Schofield (http://marine.rutgers.edu/mrs/).
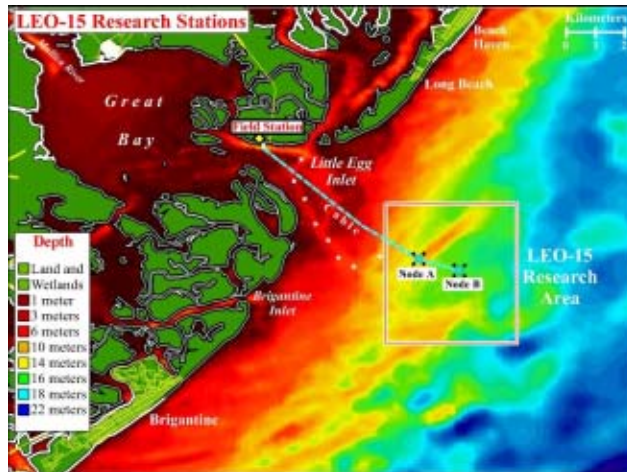
***Figure 2. The LEO-15 study site off the New Jersey coast showing Node
and field station locations superimposed on bathymetry.
(Image credit: http://marine.rutgers.edu/mrs).***

***Figure 3. A. Shalapyonok with FlowCytobot in its pressure housing
and deployment frame, after testing off the WHOI dock***

FLOWCYTOBOT SPECIFICATIONS

Divers clamped the FlowCytobot (in a protective aluminum frame; Fig. 3) to a
platform anchored to the bottom, and connected it to a Guest Node at LEO-15. A
submersible pump drew seawater from 5-m depth at a rate of 1 liter min^{-1} through a 0.5
inch tube suspended from a subsurface float and screened with 2-mm copper mesh to
prevent clogging. A programmable syringe pump with a distribution valve samples the
seawater flow through an 80 μm nylon mesh and injects the sample into the center of a
sheath of particle-free seawater flowing at a rate of 5 ml min^{-1} through a flow cell with
dimensions 180 x 400 μm. The distribution valve allows access to several reservoirs
inside the instrument. Plastic microspheres are injected periodically to monitor
performance, azide is added to sheath to prevent internal fouling, and detergent can be
added to the flow cell and tubing (during this operation, the sheath pump is stopped and

3

the laser is blocked by a hydraulically-operated shutter). The seawater sheath fluid is circulated continuously through a 0.2 μm cartridge filter by a miniature gear pump; the excess volume due to injection of sample overflows to the outside of the pressure housing. Sample injection rate is adjusted (here, 12.5 to 50 μl min^{-1}, using a 0.25-ml syringe) so that the particles in the sample pass one at a time through a laser beam from a 532 nm diode-pumped solid-state laser (100mW). A vertical beam expander followed by a 20-mm focal length spherical lens provides an elliptical laser beam spot at the flow cell. The laser beam steering mirror is under remote control to allow alignment in situ. The optical signals (forward and side light scattering, (532 nm), chlorophyll fluorescence (680 nm), and phycoerythrin fluorescence (575 nm)) are collected, separated, and detected with lenses, dichroic mirrors, and photomultipliers (PMTs) similar to those in conventional flow cytometers. The measurements have approximately 4 decades of dynamic range. A microcomputer in FlowCytobot controls the valve and pumps, acquires the optical signals, and transmits data to a shore-based computer. A more detailed description of the instrument is provided by Olson et al. (2002).

DATA ANALYSIS

For data processing and analysis, we subdivided the record of light scattering and fluorescence signals into one-hour intervals. For each interval, we used a sequence of automated steps to classify particles into one of four groups (Synechococcus, Cryptophytes, and other eukaryotes in large and small size classes) on the basis of signal characteristics (Fig. 4). Absolute cell concentrations were determined from sample pump rate and data acquisition time. We normalized all signal sizes to those from standard microspheres (1 μm), which were automatically analyzed approximately once per day during the sampling period. Cell concentration (cells ml^{-1}) for each hour was calculated from the number of cells measured and the pump rate. We estimated the volume of each phytoplankton cell using an empirical relationship between cell volume and side light scattering determined for a variety of phytoplankton species (Fig. 5).

TIME SERIES OF CELL CONCENTRATION AND SIZE

During the sampling at LEO-15, large changes in cell concentration (~2 orders of magnitude) were observed for all phytoplankton groups, and these changes were sometimes associated with shifts in water properties (Fig. 6). Unraveling the underlying causes of concentration changes such as these is a complicated problem due to the interrelated physiological, ecological, and physical processes that impact plankton concentration (e.g., Platt and Denman 1975; Steele 1978). On the biological side, phytoplankton cell division is offset by mortality due to trophic interactions such as grazing and viral lysis. If physical conditions are stable, the phasing of many phytoplankton growth processes to the daily light-dark cycle (Chisholm 1981; Prézelin 1992) may allow growth and grazing rates to be estimated from diel cell concentration changes (André et al. 1999). Stability is the exception, however, especially in coastal waters where physical processes can be a dominant source of variability in phytoplankton biomass, and we did not observe diel variance peaks in cell concentrations at LEO-15.
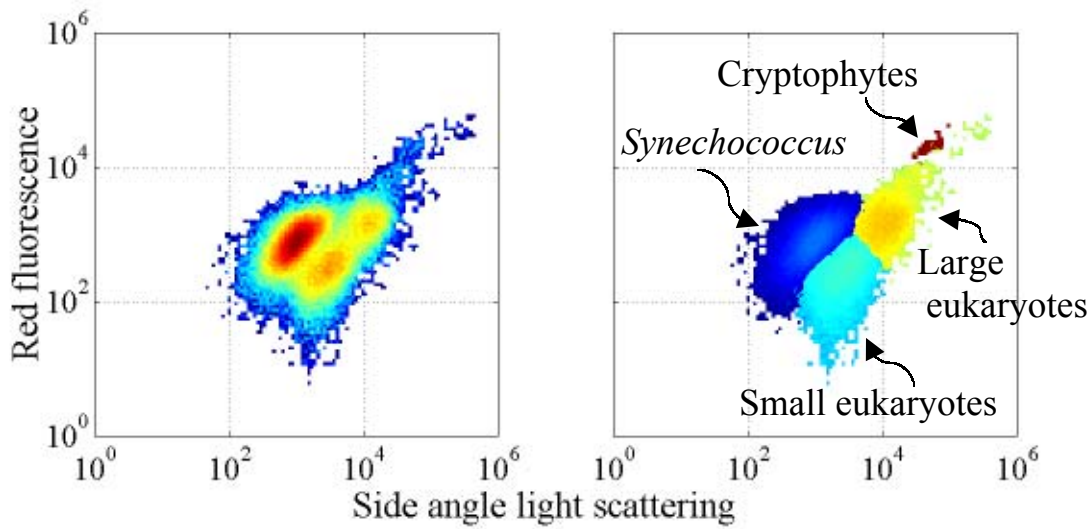
Figure 4. Two-dimensional histograms of FlowCytobot measurements from 1 hour of sampling at LEO-15. As shown in the right panel, automated classification techniques (using light scattering, and red and orange fluorescence) allow the phytoplankton assemblage to be divided into several groups: Synechococcus, cryptophytes, and other eukaryotes in large and small size classes.
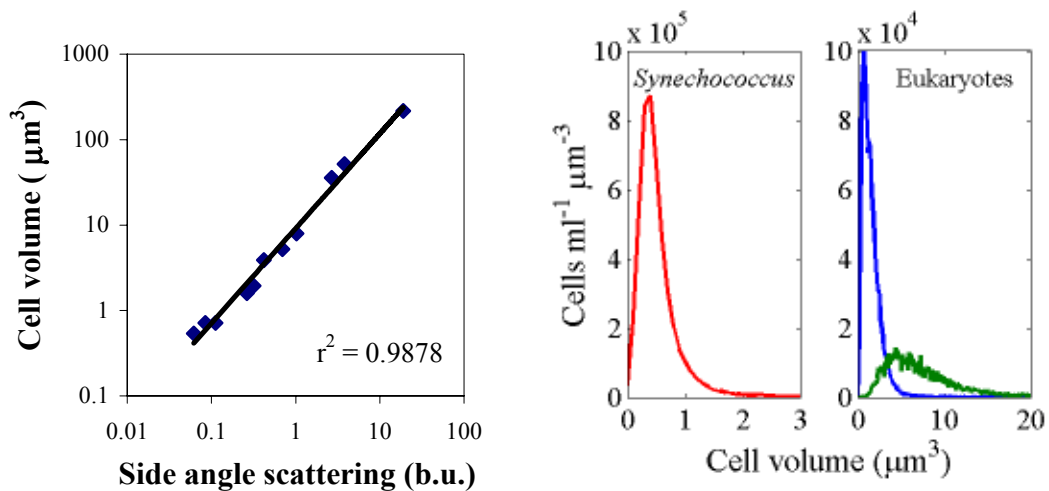

Figure 5. Empirical cell size to light scattering relationship derived from cultures of various phytoplankton species (left), and example cell volume distributions for LEO-15 waters derived from the FlowCytobot data shown in Fig. 4. The empirical relationship was determined from 11 monospecific cultures of phytoplankton (ranging in diameter from ~1 to 10 µm) grown in the laboratory and analyzed with a Coulter Multisizer and with FlowCytobot. A power law function explained 99% of the variance between cell volume and side angle light scattering.
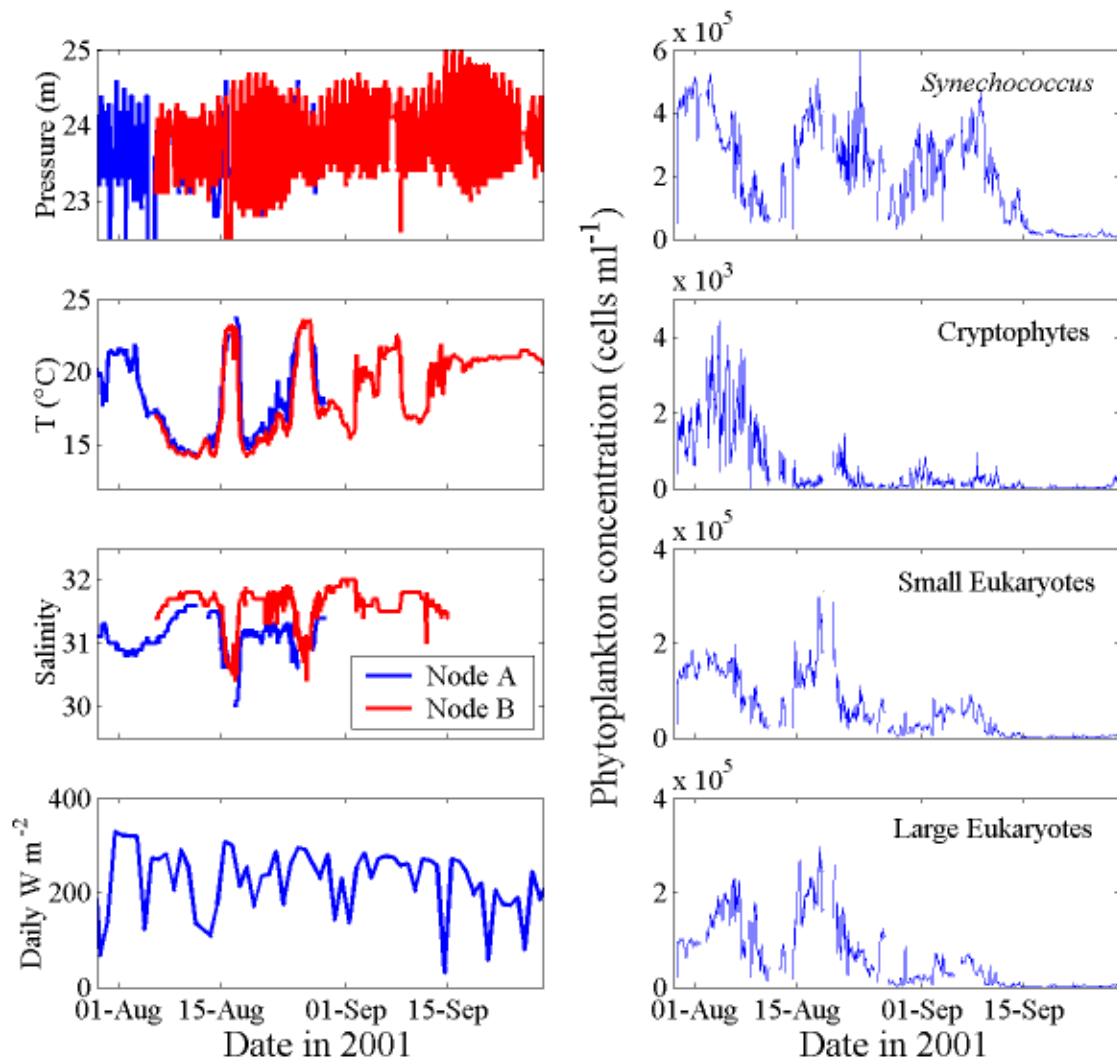
Figure 6. Time series of bottom water properties (pressure, T, S), daily solar radiation, and phytoplankton concentrations for late July through September 2001 at LEO-15. (Pressure at Node A is shown offset by 2.8 m.)

In addition to cell concentration, however, FlowCytobot measurements also provide information about phytoplankton cell size. At diel time scales, we observed distinct patterns in cell size, with cell volume generally increasing during the day and decreasing during the night at LEO-15 (Fig. 7). These patterns presumably reflect cell growth and division, as discussed elsewhere (Olson et al. 1990; Durand and Olson 1996; Shalapyonok et al. 1998; Jacquet et al. 2001). If changes in population size distributions can be quantitatively related to cell growth and division, then this information can be used to separate the effects of cell division from other processes influencing cell concentration.
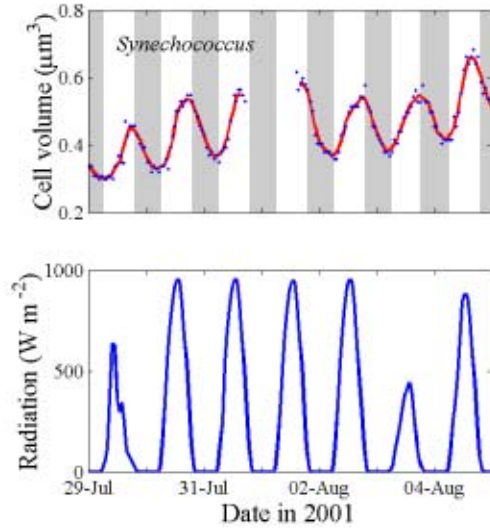
Figure 7. One week subset of the time series to show examples of the diel variations in mode cell volume exhibited by Synechococcus. Gray bars indicate nighttime.

CELL GROWTH AND DIVISION MODEL

On the basis of simple assumptions about the diel cycle of cell growth and division, a crude estimate of intrinsic growth rate can be derived from the increase in mean cell size between dawn and dusk. This approach has been used for open ocean *Synechococcus* and other phytoplankton groups (Durand 1995; Binder et al. 1996; Vaulot and Marie 1999). The major limitation of this simple approach is that it assumes that cell growth and cell division are segregated during the daily cycle. Laboratory studies of *Synechococcus*, in particular, have demonstrated that growth and division can occur simultaneously in a population (Waterbury et al. 1986; Binder and Chisholm 1995; Jacquet et al. 2001), so that the simple approach underestimates growth rate. To overcome this limitation we developed a matrix population model (Caswell 2000) that incorporates the full size distribution of the population, and accommodates simultaneous growth and division (Sosik et al. 2002). The model does not depend on measured cell concentration. We have initially developed our modeling approach for *Synechococcus* because these cells abundant were contributors to the phytoplankton community at the study site and they could be distinguished unambiguously from other taxonomic groups in our FlowCytobot data.

Under our model, changes in cell size are due to growth (which depends on light conditions) and cell division. The rate of cell loss is assumed to be independent of size. The model is based on discrete size classes; for this case we used 57 logarithmically spaced bins ranging from 0.03 to 4 μm^3. In each 10-min time step, a fraction of the cells in each size class divide, with each dividing cell producing 2 daughter cells of half the original size. The division fraction, δ, depends on cell size v as:

$$\delta = \delta_{max} \, av^b /(1 + av^b) \qquad (1)$$

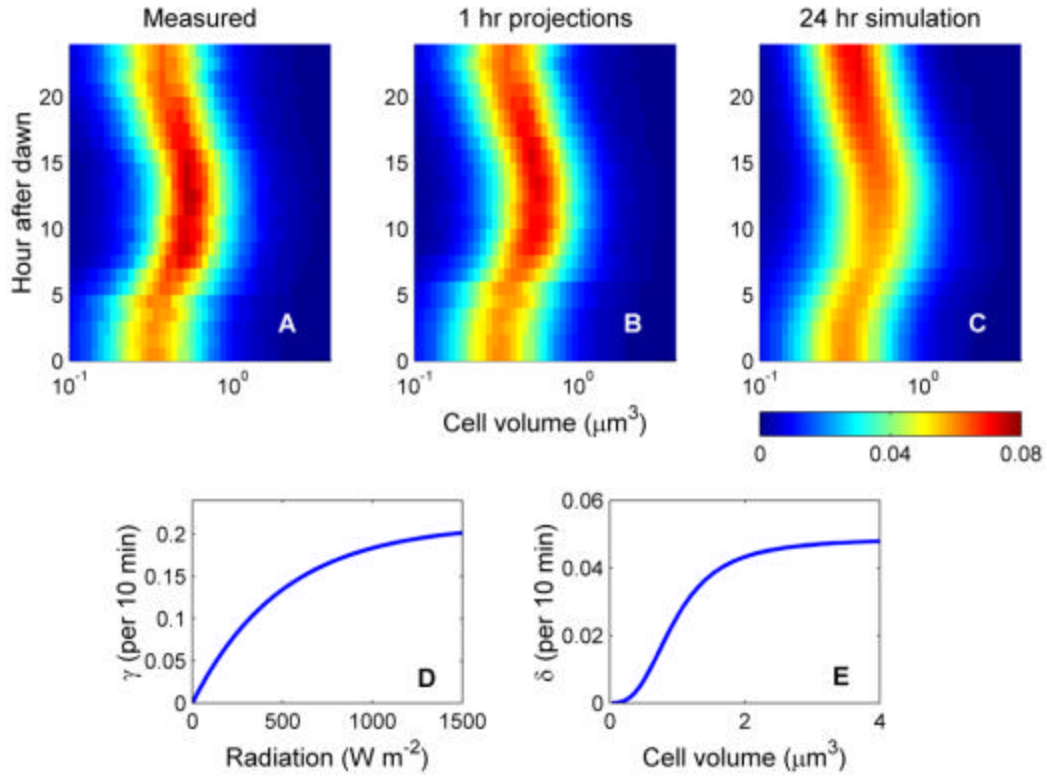(Fig. 8E). Cell division is not permitted until 6 hours after dawn. Of the cells that do not

7

*Figure 8. Measured (A) and modeled (B and C) size distributions for **Synechococcus** in surface waters of the New Jersey shelf on July 31, 2001. Size distributions are shown for each hour of the day, with the color bar indicating relative cell concentration in logarithmically spaced size classes. The 1-h model projections (B) were compared to the observed distributions (A) to determine the best-fit model parameters for each day. As detailed in the text, two parameters describe the light dependence of the fraction of cells progressing from one size class to the next (D); three other parameters describe how the fraction of cells that divide depends on cell volume (E). Even when the model (fit using 1-h projections) was used to project the initial size distribution forward over the entire day (C), the results were similar to the observations (A).*

divide at time t, a fraction $\boldsymbol{g}(t)$ grow into the next largest size class. $\boldsymbol{g}(t)$ depends on measured irradiance $E(t)$ as:

$$\boldsymbol{g}(t) = \boldsymbol{g}_{\max}\left[1 - \exp\left(E(t)/E_k\right)\right] \tag{2}$$

(Fig. 8D). Cells that neither divide nor grow remain in the same size class.

We estimated the model parameters $\boldsymbol{d}_{\max}$, a, b, $\boldsymbol{g}_{\max}$, and E_k for each day (dawn to dawn) by minimizing the weighted sum of squared deviations between the observed and modeled size distributions in 1-h intervals, where the weights were the sample sizes in each hour (Fig. 8A-C). The intrinsic growth rate within a day is given by the model

predicted change in cell concentration (due to cell division in the absence of cell loss) over the course of the day.

SYNECHOCOCCUS GROWTH RATES

From our data and model results we derived a time series of population growth rate for *Synechococcus*. These results suggest that physical processes caused the observed *Synechococcus* population decline during early August (Fig. 9A). There is no evidence that the decline was associated with a decrease in intrinsic growth before or during this period (Fig. 9B). As a consequence, cell specific loss rate must have increased (Fig. 9C). While we cannot unambiguously distinguish between biological losses, such as grazing, and losses due to physical transport of cells, other evidence suggests that physical processes played an important role in the observed population decline. Bottom water temperatures at LEO-15 experienced a ~8 °C drop during this period (Fig. 6B), which was most likely due to upwelling of deeper, colder shelf waters forced by the predominantly southwesterly winds. Wind-driven upwelling is common in this area, and has previously been reported to bring in water masses with higher chlorophyll concentration and particle load (Glenn et al. 2000; Schofield et al. 2002). In 2001, however, a series of upwelling events similar to the one we observed in August occurred earlier in the summer, and these earlier events were accompanied by lower turbidity at LEO-15 (O. Schofield, personal communication), which is consistent with our observation of low phytoplankton concentration. Later in August, another apparent upwelling event and major changes in cell concentration were observed (Fig. 2), but without the same association. These results underscore the complexity of predicting consequences of events like upwelling on plankton distributions, and emphasize the need for combined physical and biological time-series observations.

The largest change we observed in *Synechococcus* concentration occurred in mid-September (Fig. 9A). In contrast to the population decline in early August, this dramatic decline appears to have had a physiological cause. During the September decline cell-specific loss rates did not increase, but intrinsic growth rates decreased (Fig. 9A,B). Intrinsic growth rates were high at the end of August and in the beginning of September, with cells consistently dividing more than once per day. Then, over four days beginning on September 7, growth rates dropped from >0.9 to <0.2 d^{-1}. Possibly due to light limitation (Sosik et al. 2002), growth rates stayed well below one doubling per day (i.e., < 0.69 d^{-1}) for the remainder of September, while cell concentrations fell from >4 x 10^5 to <8 x 10^3 ml^{-1} and never recovered (Fig. 9A).
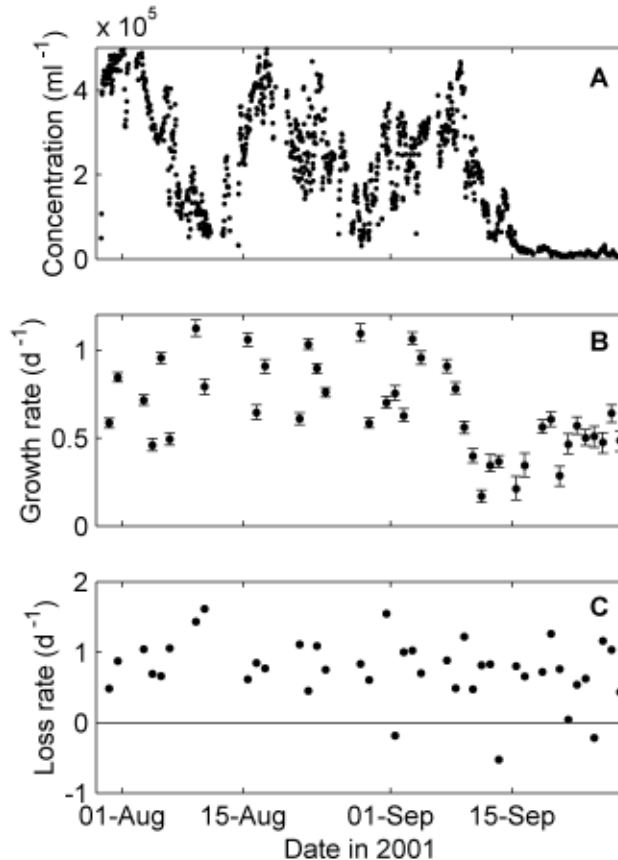
Figure 9. Time series of Synechococcus population properties in surface waters of the New Jersey shelf. Cell concentrations with 1-h resolution (A) were determined directly from FlowCytobot measurements. Daily intrinsic growth rates of Synechococcus (B) were determined from measured cell size distributions and a linear matrix model for cell growth and division over the diel cycle. Error bars represent 95% confidence intervals estimated from 1000 bootstrapped data sets. Apparent cell-specific loss rates (C) were estimated by difference between the intrinsic growth rates and the observed daily rates of population increase calculated directly from the concentrations in panel A. Grazing by microzooplankton would contribute to positive loss rates, while physical processes, including water mass mixing and advection, could result in positive or negative loss rates.

CONCLUSIONS

Our initial work with submersible automated flow cytometry has demonstrated the kinds of insights into phytoplankton dynamics that this technology can facilitate, especially in combination with modeling such as we have proposed to describe changes in cell size. The fundamental response of a plankton population to environmental change is expressed in its intrinsic growth rate, but growth rates in the dynamic coastal ocean cannot be determined from traditional measurements of pigment biomass or even cell abundance. Population modeling that uses time series of cell size data from automated instrumentation has enabled us to estimate growth rates, and thus to distinguish

10

physiologically-driven change in phytoplankton abundance from more incidental fluctuations; for *Synechococcus* on the New Jersey shelf, both growth rate changes and physical processes combined with spatial patchiness are important at different times. Distinguishing between these sources of variability is crucial for understanding the regulation of coastal ecosystems. We expect that new insights will continue to be revealed as automated flow cytometers such as FlowCytobot and the independently developed "CytoBuoy" (Dubelaar et al. 1999) are incorporated into plans for interdisciplinary coastal ocean monitoring systems (e.g., Malone and Cole 2000).

REFERENCES

André, J.-M., C. Navarette, J. Blanchot, and M.-H. Radenac. 1999. Picophytoplankton dynamics in the equatorial Pacific: Growth and grazing rates from cytometric counts. Journal of Geophysical Research **104:** 3369-3380.

Binder, B. J., and S. W. Chisholm. 1995. Cell cycle regulation in marine Synechococcus sp. strains. Applied and Environmental Microbiology **61:** 708-717.

Binder, B. J., S. W. Chisholm, R. J. Olson, S. L. Frankel, and A. Z. Worden. 1996. Dynamics of picophytoplankton, ultraphytoplankton and bacteria in the Central Equatorial Pacific. Deep-Sea Research (Part 2, Topical Studies in Oceanography) **43:** 907-931.

Caswell, H. 2000. Matrix Population Models, 2 ed. Sinauer.

Chisholm, S. W. 1981. Temporal Patterns of Cell Division in Unicellular Algae, p. 150-181. *In* T. Platt [ed.], Physiological Bases of Phytoplankton Ecology. Can. Bull. Fish. Aquat. Sci.

Dickey, T. 1991. The emergence of concurrent high-resolution physical and bio-optical measurements in the upper ocean and their applications. Reviews of Geophysics **29:** 383-413.

---. 2001. New technologies and their roles in advancing recent biogeochemical studies. Oceanography **14:** 108-120.

Dubelaar, G. B. J., P. L. Gerritzen, A. E. R. Beeker, R. R. Jonker, and K. Tangen. 1999. Design and First Results of CytoBuoy: A Wireless Flow Cytometer for In Situ Analysis of Marine and Fresh Waters. Cytometry **37:** 247-254.

DuRand, M. D. 1995. Phytoplankton growth and diel variations in beam attenuation through individual cell analysis, p. 267. Massachusetts Institute of Technology, Woods Hole Oceanographic Institution.

DuRand, M. D., and R. J. Olson. 1996. Contributions of phytoplankton light scattering and cell concentration changes to diel variations in beam attenuation in the equatorial Pacific from flow cytometric measurements of pico-, ultra- and nanoplankton. Deep-Sea Research (Part 2, Topical Studies in Oceanography) **43:** 891-906.

Glenn, S. M., W. Boicourt, B. Parker, and T. D. Dickey. 2000. Operational Observation Networks for Ports, a Large Estuary and an Open Shelf. Oceanography **13:** 12-23.

Jacquet, S., F. Partensky, J. Lennon, and D. Vaulot. 2001. Diel Patterns of Growth and Division in Marine Picoplankton in Culture. Journal of Phycology **37:** 357-369.

Malone, T. C., and M. Cole. 2000. Toward a Global Scale Coastal Ocean Observing System. Oceanography **13:** 7-11.

Olson, R. J., S. W. Chisholm, E. R. Zettler, and E. V. Armbrust. 1990. Pigments, size, and distribution of *Synechoccus* in the North Atlantic and Pacific Oceans. Limnology and Oceanography **35(1):** 45-58.

Olson, R. J., A. A. Shalapyonok, and H. M. Sosik. 2002. An automated submersible flow cytometer for pico- and nanophytoplankton: FlowCytobot. Deep-Sea Research (Part 1, Oceanographic Research Papers). submitted.

Platt, T., and K. L. Denman. 1975. Spectral analysis in ecology. Annual Review of Ecology and Systematics **6:** 189-210.

Prézelin, B. B. 1992. Diel periodicity in phytoplankton productivity. Hydrobiologia **238:** 1-35.

Schofield, O., T. Bergmann, W. P. Bissett, F. Grassle, D. Haidvogel, J. Kohut, M. Moline, and S. Glenn. 2002. Linking regional coastal observatories to provide the foundation for a national ocean observation network. IEEE Journal of Oceanic Engineering. in press.

Shalapyonok, A. A., R. J. Olson, and L. S. Shalapyonok. 1998. Ultradian Growth in Prochlorococcus spp. Applied and Environmental Microbiology **64:** 1066-1069.

Sosik, H. M., R. J. Olson, M. G. Neubert, A. A. Shalapyonok, and A. R. Solow. 2002. Intrinsic growth rates in coastal phytoplankton populations from time-series measurements with a submersible flow cytometer. Proceedings of the National Academy of Science USA. submitted.

Steele, J. H. 1978. Spatial pattern in plankton communities, p. 470. Plenum.

Vaulot, D., and D. Marie. 1999. Diel variability of photosynthetic picoplankton in the equatorial Pacific. Journal of Geophysical Research **104:** 3297-3310.

Waterbury, J. B., S. W. Watson, F. W. Valois, and D. G. Franks. 1986. Biological and ecological characterization of the marine unicellular cyanobacterium *Synechococcus*, p. 71-120. *In* T. Platt and W. K. W. Li [eds.], Photosynthetic Picoplankton, Can. Bull. Fish. Aquat. Sci.